journal

J. Am. Ceram. Soc., 1–5 (2012)
DOI: 10.1111/j.1551-2916.2012.05294.x

Dielectric and Relaxor Properties of $Ba_9MNb_{14}O_{45}$ Ceramics

Oleg Ovchar,[‡,†] Dmitrii Durilin,[‡] Anatolii Belous,[‡] Boštjan Jančar,[§] and Taras Kolodiazhnyi[¶]

[‡]Department of Solid State Chemistry, V.I.Vernadskii Institute of General and Inorganic Chemistry NAS of Ukraine, Kyiv 03680, Ukraine

[§]Advanced Materials Department, "Jožef Stefan" Institute, Ljubljana 1000, Slovenia

[¶]National Institute for Materials Science, Tsukuba, Ibaraki 305-0044, Japan

The ceramics with two types of nominal compositions including (6:1:4.5) $Ba_6M^{2+}Nb_9O_{29.5}$ and (9:1:7) $Ba_9M^{2+}Nb_{14}O_{45}$ (M = Mg, Co, Zn) have been synthesized and studied with regard to their phase composition and dielectric properties. The materials with $Ba_6M^{2+}Nb_9O_{29.5}$ nominal compositions corresponded to the two-phase region containing 9:1:7 tetragonal tungsten bronze-type (TTB) phase and the 3:1:1 perovskite $Ba(M^{2+}_{1/3}Nb_{2/3})O_3$. In contrast, 9:1:7 TTB ceramics were near single phase. All of the studied 9:1:7 TTB phases exhibited high values of dielectric permittivity (ε = 800–1100) together with strong frequency dispersion. The observed dispersion of permittivity was accompanied by the monotonic rise of dielectric loss. The dielectric spectra of 9:1:7 TTBs demonstrated a typical relaxor behavior. At low temperatures (100–300 K), two relaxation modes have been found in the tan δ (*T*) dependencies, which can be associated with two different types of structural disorder in the TTB crystal lattice.

I. Introduction

Recently, ceramics based on the $BaO–M^{2+}O–Nb_2O_5$ ternary system (M = Co, Zn, Mg) have been attracting sustainable interest as dielectric materials suitable for microwave (MW) applications.[1] In this regard, the most studied compositions of the above system are 3:1:1 complex perovskites $Ba(M^{2+}_{1/3}Nb_{2/3})O_3$, which display extremely high values of the quality factor (Q = 1/tan δ) in the centimeter and millimeter wavelength bands.[2–4] For example, a $Q \times f$ product as high as 230 000 GHz at frequencies above 60 GHz has been reported for $Ba(Mg_{1/3}Nb_{2/3})O_3$ ceramics.[5]

As a rule, high magnitudes of the Q-factor in $Ba(M^{2+}_{1/3}Nb_{2/3})O_3$ perovskites are generally attributed to the 1:2 ordered B-sublatice, which comprises single layers of M^{2+} cations alternating with double layers of Nb^{5+} cations perpendicular to the <111> direction of the pseudocubic cell.[6,7] Cation ordering in $Ba(M^{2+}_{1/3}Nb_{2/3})O_3$ is a kinetically driven process, which can be significantly accelerated by a slight deficiency in cation sublattices.[4,8] In this case, the highest Q-factors have been obtained in A-site deficient single-phase $Ba(Mg_{1/3}Nb_{2/3})O_3$ (BMN)[4,5] and $Ba(Zn_{1/3}Nb_{2/3})O_3$ (BZN).[8] However, in both compositions, the increase in the Q-factor magnitude was always followed by its abrupt fall at higher Ba deficiency that has been attributed to the effect of the secondary phase with the tetragonal tungsten bronze (TTB) structure.[4,9] The presence of the TTB phase has been detected also in the Ba-deficient $Ba(Co_{1/3}Nb_{2/3})O_3$ (BCN), which demonstrated a very similar behavior of the Q-factor.[9] According to the EDX/WDS analysis, the compositions of these secondary TTB phases were rich in Nb, and contained lower concentration of M^{2+} in comparison with the main perovskite phase.[9] However, due to a rather scarce amount of the TTB phases in the studied materials their exact compositions could not be accurately determined.

Moreover, the literature data on the ternary TTB phases that form in the vicinity of a 3:1:1 perovskite are quite contradictory. On the one hand, there are several reports on the formation of 9:1:7 phases $Ba_9M^{2+}Nb_{14}O_{45}$, with M^{2+} = Co[10] and Zn,[11] further referred to the solid solutions with general formula $Ba_{5+5x}M^{2+}{}_{10x/3}Nb_{10-10x/3}O_{30}$ for x = 0.20–0.19 (T. A. Vanderah, E. Pickett, I. Levin, and R. S. Roth, National Institute of Standards and Technology, private communication, Gaithersburg, MD, 2005). On the other hand, several authors reported on the formation of the TTB phase $Ba_6CoNb_9O_{30}$.[12,13] The latter one implies that all Co ions are in a Co (III) oxidation state. This is a highly unlikely situation in ceramics sintered well above 950°C, when mixed-valence Co (II, III) oxide Co_3O_4 transforms to a stable Co (II) oxide CoO. Moreover, neither the phase composition nor the Co valence has been carefully studied in Refs. [12] and [13].

Also, the dielectric properties of the 9:1:7 TTB phases have not yet been studied. There is only one recent report on the room-temperature dielectric parameters of Mg-containing 9:1:7 TTB phase $Ba_9MgNb_{14}O_{45}$ denoting the large dielectric constant with a very strong frequency dependence and large dielectric loss.[14] At the same time, the properties of Co-containing TTB phase $Ba_6CoNb_9O_{30}$ are again quite contradictory. In the Ref. [12], this phase is considered as the ferroelectric compound with a diffuse phase transition at 660 K and a room-temperature spontaneous polarization of 2.2×10^{-2} Cm^{-2}, whereas the authors of Ref. [13] found a broad permittivity maximum that shifts in the temperature range from 140 K (5 Hz) to 225 K (1 MHz), denoting a typical ferroelectric relaxor behavior of $Ba_6CoNb_9O_{30}$. Furthermore, a nonlinear soft magnetic behavior has also been found in $Ba_6CoNb_9O_{30}$, and was attributed to the presence of Co^{3+} ions.[13] More careful literature analysis reveals that the ferroelectric relaxor behavior, very similar to that of $Ba_6CoNb_9O_{30}$, was previously found in the Ba-deficient perovskite BMN, which was considered as a single-phase compound.[15] However, according to our recent studies on Ba-deficient $Ba(M^{2+}_{1/3}Nb_{2/3})O_3$,[4] BMN perovskites reported in Ref. [15] must have contained a certain amount of secondary TTB phase.

Taking into account all the above listed shortages and inconsistencies, we report here on the compositions and dielectric properties of the TTB phases found in the vicinity of the 3:1:1 perovskites $Ba(M^{2+}_{1/3}Nb_{2/3})O_3$ (M^{2+} = Mg, Co, Zn). We believe that these findings are important for

P. K. Davies—contributing editor

Manuscript No. 31024. Received February 01, 2012; approved April 27, 2012.
[†]Author to whom correspondence should be addressed. e-mail: ovcharoleg@yahoo.com

understanding of the variation of the dielectric properties in the niobate-based high-Q microwave dielectrics.

II. Experimental Procedure

In this work, the compositions with two different ratios of starting oxides have been used to produce target TTB phases. These included (I) $6BaO–M^{2+}O–4.5\ Nb_2O_5$ and (II) $9BaO–M^{2+}O–7Nb_2O_5$ (M^{2+} = Mg, Co, Zn). The ceramics were prepared by the conventional mixed-oxide route. The starting reagents were 99.95% pure MgO, Co_3O_4, ZnO, Nb_2O_5, and $BaCO_3$. The weighted mixtures of starting reagents were calcined at 1100°C–1200°C for 4 h. The sintering was performed in air for 8 h at 1300°C–1350°C. The phase composition of sintered ceramics was examined by means of X-ray diffraction analysis (XRD) using Cu$K\alpha$ radiation (Model PW 1700; Philips, Eindhoven, The Netherlands). Microstructural analysis of the ceramic samples was performed by means of scanning electron microscopy (JSM 5800; JEOL, Tokyo, Japan) using energy-dispersive X-ray spectroscopy (EDX) and the LINK software package (ISIS 3000; Oxford Instruments, Bucks, U.K.). Room-temperature dielectric properties (ε and tan δ) were studied using Solartron 1260 A Impedance Analyzer (Solartron Analytical, Farnborough, Hampshire, U.K.), whereas low-temperature behavior was evaluated using Agilent E4980 Precision LCR Meter (Agilent Technologies Inc., Santa Clara, CA) in the temperature interval of 2.5–300 K utilizing a home-made dielectric-measurements probe coupled with the Physical Property Measurement System (Quantum Design, San Diego, CA).[16]

III. Results and Discussion

(1) System $6BaO–M^{2+}O–4.5\ Nb_2O_5$ (M^{2+} = Mg, Co, Zn)

The ceramics of this system have been produced from the stoichiometric sources of starting oxides BaO, $M^{2+}O$, and Nb_2O_5 taken in the ratio (6:1:4.5) to obtain the nominal compositions $Ba_6M^{2+}Nb_9O_{29.5}$. It should be noted here that the ratios $Ba/M^{2+}/Nb$ in starting powders were equal to those used for the preparation of $Ba_6CoNb_9O_{30}$.[12,13] However, in our study, all of the nominal compositions were calculated deriving from Co (II) oxidation state. At the same time, the preparation conditions for studied ceramics were quite similar to those described in the Refs. [12] and [13].

In contrast to the findings previously reported for $Ba_6CoNb_9O_{30}$, independent on the M^{2+} species we did not obtain a single-phase composition.[12,13] According to the analysis of the X-ray diffraction patterns (2Θ = 20°–35°) collected from sintered and crushed ceramics with the nominal compositions $Ba_6M^{2+}Nb_9O_{30}$ (M^{2+} = Mg, Co, Zn), the peaks' positions match those of the PDF 73-1879 ($Ba_6CoNb_9O_{30}$) except for one unidentified peak in the vicinity of 2Θ = 30.7°–30.8° (Fig. 1). The presence of this peak on the XRD patterns clearly denotes the existence of the additional phase in the ceramics with the nominal compositions $Ba_6M^{2+}Nb_9O_{30}$ (M^{2+} = Mg, Co, Zn).

It is interesting to note that, when analyzing the XRD pattern of the "$Ba_6CoNb_9O_{30}$" ceramics, the authors of the Ref. [13] also reported the presence of an additional XRD peak with a similar intensity at the same 2Θ range. However, this peak has been attributed to the minor amount of $Ba_{1.04}NbO_3$ phase, implying the presence of not only Co (III) but also Nb (IV). Unfortunately, these conclusions were not anyhow further confirmed in Ref. [13] from the experimental data. We highly doubt that both Co (III) and Nb(IV) can coexist during the synthesis in air. Although the former species would require highly oxidizing conditions to form, the latter species would require extremely reducing conditions (for example, synthesis in hydrogen or high vacuum). In our study, the phase content of the $Ba_6M^{2+}Nb_9O_{29.5}$ ceramics has been identified by the detailed SEM analysis (Fig. 2).

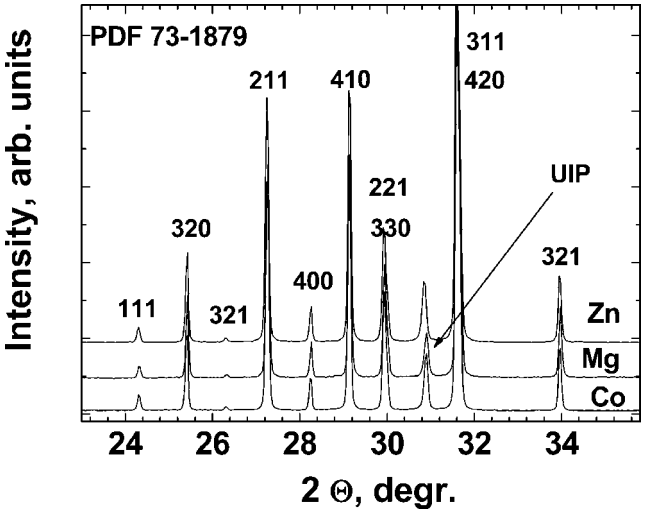

Fig. 1. XRD patterns of the crushed ceramics (I) with the nominal composition $6BaO–M^{2+}O$- 4.5 Nb_2O_5 (6:1:4.5) for M^{2+} = Mg, Zn, Co indexed in accordance with the PDF 73-1879. UIP is a "surplus" unidentified peak at 2Θ = 30.7°–30.8°.

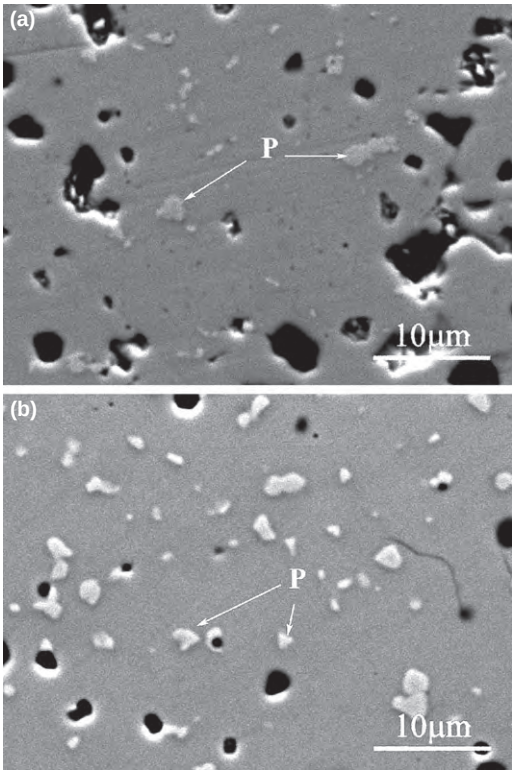

Fig. 2. SEM microphotographs of the polished surface of the $Ba_6M^{2+}Nb_9O_{29.5}$ Ceramics (a) M^{2+} = Co; (b) M^{2+} = Mg. P = $Ba(M^{2+}{}_{1/3}Nb_{2/3})O_3$.

According to the EDS data, the compositions of the observed secondary phases were close to $Ba(M^{2+}{}_{1/3}Nb_{2/3})O_3$ cubic perovskite, which in the case of M^{2+} = Mg or Zn fits well with the corresponding phase diagrams (T. A. Vanderah, E. Pickett, I. Levin, and R. S. Roth, National Institute of Standards and Technology, private communication, Gaithersburg, MD, 2005). At the same time, the compositions of the matrix phases were close to the 9:1:7 TTB phase $Ba_9M^{2+}Nb_{14}O_{45}$.

Therefore, the unidentified peaks found at 2Θ = 30.7°–30.8° most likely correspond to the most intense (110) peaks of the perovskites $Ba(M^{2+}{}_{1/3}Nb_{2/3})O_3$. Other intense peaks merely overlap with the peaks of the TTB phase (Fig. 1).

Table I. Room-Temperature RF Dielectric Parameters of $Ba_6M^{2+}Nb_9O_{29.5}$ and $Ba_9M^{2+}Nb_{14}O_{45}$ Ceramics

	$Ba_6M^{2+}Nb_9O_{29.5}$			$Ba_9M^{2+}Nb_{14}O_{45}$		
M^{2+}	Phase composition	ε (1 MHz)	tan δ (1 MHz)	Phase composition	ε (1 MHz)	tan δ (1 MHz)
Co	9:1:7 TTB + perovskite	340	5.0×10^{-3}	9:1:7 TTB	800	3.8×10^{-2}
Mg	9:1:7 TTB + perovskite	400	2.0×10^{-3}	9:1:7 TTB	1000	2.0×10^{-2}
Zn	9:1:7 TTB + perovskite	550	6.8×10^{-3}	9:1:7 TTB	1100	0.12

As a consequence of our findings, we can conclude that the ceramics with the nominal compositions $Ba_6MNb_9O_{29.5}$ (M = Mg, Co, Zn) are mainly a mixture of two crystalline phases: the matrix 9:1:7 TTB phase and the cubic perovskite $Ba(M^{2+}{}_{1/3}Nb_{2/3})O_3$. To be more accurate, according to the ternary phase rule, the $Ba_6MNb_9O_{29.5}$ ceramics should consist of three phases. However, because the $Ba_6MNb_9O_{29.5}$ nominal composition is located very close to the tie line connecting the $Ba(M^{2+}{}_{1/3}Nb_{2/3})O_3$ and $Ba_9M^{2+}Nb_{14}O_{45}$ phases, the amount of the third phase appears to be negligible. According to the BaO–ZnO(MgO)–Nb_2O_5 ternary phase diagrams (T. A. Vanderah, E. Pickett, I. Levin, and R. S. Roth, National Institute of Standards and Technology, private communication, Gaithersburg, MD, 2005), the third phase in the $Ba_6ZnNb_9O_{29.5}$ and $Ba_6MgNb_9O_{29.5}$ compositions should correspond to ZnO and MgO phases, respectively. The lack of information about the BaO–CoO–Nb_2O_5 ternary phase diagram does not allow us to estimate to nature of the third phase that should exist in the $Ba_6CoNb_9O_{29.5}$ composite compound.

The room-temperature dielectric properties of the $Ba_6MNb_9O_{29.5}$ composites measured at around 1 MHz are presented in the Table I. One can see from the table, that in the case of $Ba_6CoNb_9O_{29.5}$ ceramics, the data correspond well to those presented in Ref. [13]. At the same time, the extended discussion in Ref. [13] on the role of Co^{3+} in dielectric and magnetic properties of $Ba_6CoNb_9O_{30}$ seems to have less ground, assuming that the presence of Co(III) in the ceramics was not clearly proved. Most likely, the reported properties can be attributed to the effect of the matrix 9:1:7 TTB phase.

(2) System $9BaO–M^{2+}O–7Nb_2O_5$ (M^{2+} = Mg, Co, Zn)

In this system, regardless of the M^{2+} species, nearly single-phase ceramics have been produced. The X-ray diffraction patterns of sintered $Ba_9M^{2+}Nb_{14}O_{45}$ (Fig. 3) correspond well to a single-phase TTB (PDF 50-1884 and/or 51-1869).

These data are confirmed using electron microscopy, which denotes the negligible amount of secondary hexagonal perovskite $Ba_5Nb_4O_{15}$ (Fig. 4). The concentration of $Ba_5Nb_4O_{15}$ in the M^{2+} = Zn ceramics is slightly higher, which can be attributed to the ZnO evaporation at sintering temperature.

At room temperature, all the studied 9:1:7 TTB phases exhibit high values of dielectric permittivity which are within the range ε = 700–1000 at the frequency 1 MHz, and which slightly increase with the ionic radii of M^{2+} [Table I, Fig. 5(a)]. Also, the TTB phases demonstrate strong frequency dispersion of permittivity, which is the most pronounced in the case of $Ba_9ZnNb_{14}O_{45}$. The observed dispersion of permittivity is accompanied by the monotonic rise of dielectric loss [Table I, Fig. 5(b)].

Low-temperature measurements of the dielectric spectra of $Ba_9M^{2+}Nb_{14}O_{45}$ (Fig. 6) demonstrate a typical relaxor behavior of all studied TTB compounds. The broad maxima on the dependencies of ε (T) and tan δ (T) have been found around 200–250 K and 100–200 K, respectively, in the case of M^{2+} = Co, Mg, and around 250–300 K (ε) and 100–300 K (tan δ) in the case of M^{2+} = Zn. At a fixed frequency, the temperatures corresponding to the maxima of ε and tan δ (T_M) increase with increasing ionic radii of M^{2+} (Fig. 6). In general, the dielectric spectra of $Ba_9M^{2+}Nb_{14}O_{45}$ indicate a broad distribution of the relaxation times, denoting a high structural disorder of the studied TTB compounds.[17]

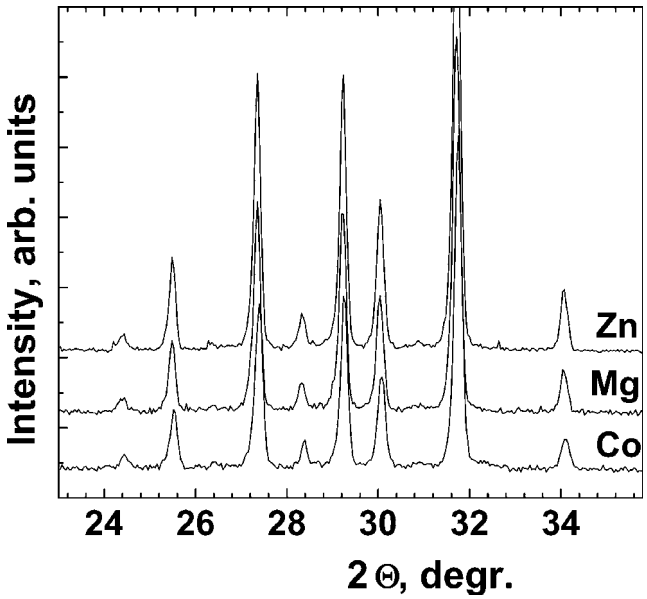

Fig. 3. XRD patterns collected on the crushed powder of sintered samples $Ba_9M^{2+}Nb_{14}O_{45}$ (M^{2+} = Co, Zn, Mg).

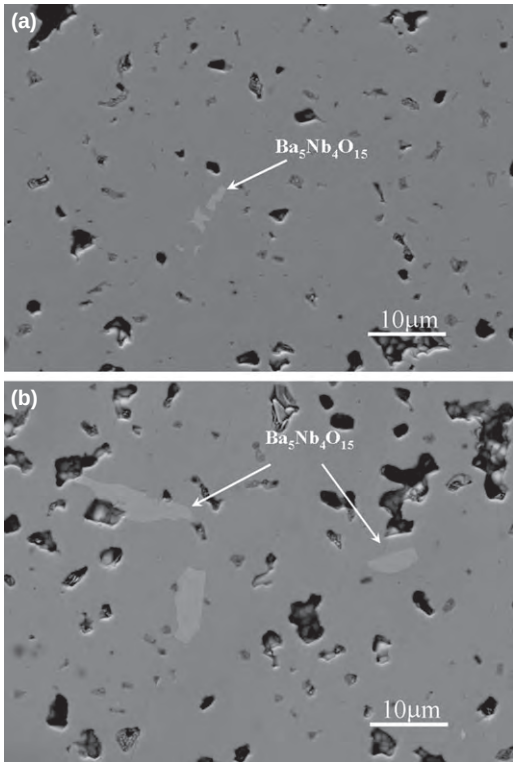

Fig. 4. SEM microphotographs of the polished surface of sintered samples $Ba_9M^{2+}Nb_{14}O_{45}$. (a) M^{2+} = Co; (b) M^{2+} = Zn.

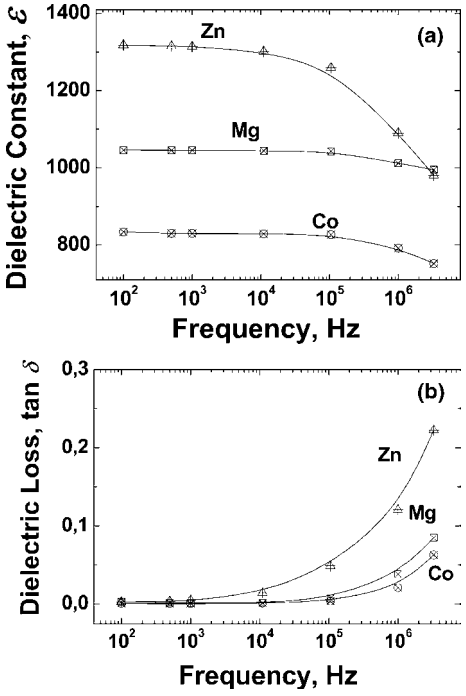

Fig. 5. Room-temperature frequency dependencies of the permittivity (a) and dielectric loss (b) of sintered $Ba_9M^{2+}Nb_{14}O_{45}$; M^{2+} = Co, Mg, Zn.

However, it should be noted that in the case of M^{2+} = Co or Zn, one can clearly distinguish two different relaxation modes in the tan δ (T) dependence. In contrast, in the case of M^{2+} = Mg these modes are overlapped, and hence cannot be easily separated. Both the modes in $Ba_9M^{2+}Nb_{14}O_{45}$ (except for $Ba_9MgNb_{14}O_{45}$) can be modeled in accordance with the Arrhenius-type equation:

$$f = f_\infty \exp\left(\frac{-E_A}{kT}\right),$$

where f_∞ is the relaxation frequency at infinite temperature, E_A is the temperature-independent activation energy, and k – is the Boltzmann constant.[17] The use of the Vogel–Fulcher relation

$$f = f_\infty \exp\left(\frac{-E_A}{k(T - T_{VF})}\right),$$

where T_{VF} is the finite "freezing" temperature, gives close to zero T_{VF}, and hence transforms again to the Arrhenius law. From the Arrhenius plots for $Ba_9M^{2+}Nb_{14}O_{45}$ (M^{2+} = Co, Zn) one can see that both the relaxation modes demonstrate a very similar behavior regardless of the type of the M^{2+} species (Fig. 7). The relaxation parameters (E_a and f_∞) of the Arrhenius fitting for $Ba_9M^{2+}Nb_{14}O_{45}$ are summarized in the Table II. Beyond the physical meaning of the calculated parameters, one can see a significant difference between the temperature dependence of the two fitted modes, which may

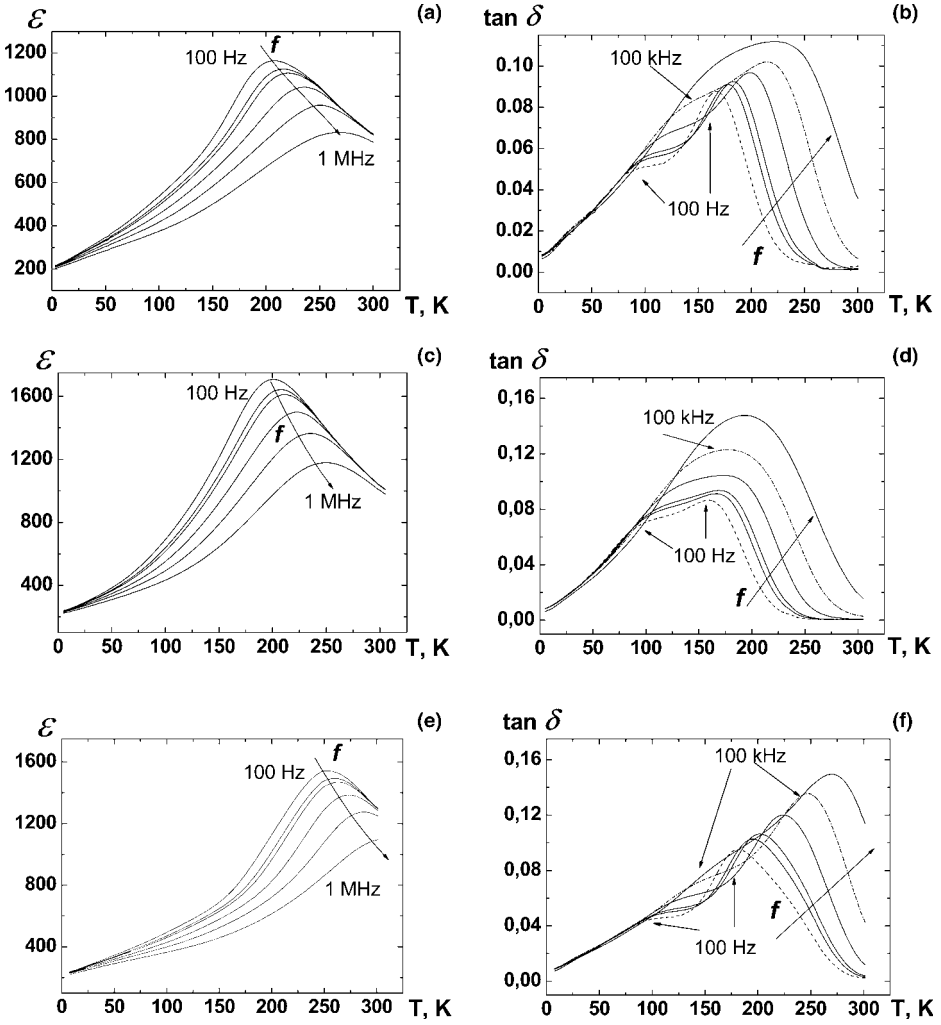

Fig. 6. Low-temperature dielectric spectra of $Ba_9M^{2+}Nb_{14}O_{45}$ Ceramics; M^{2+} = Co (a, b), Mg (c,d), Zn (e, f).

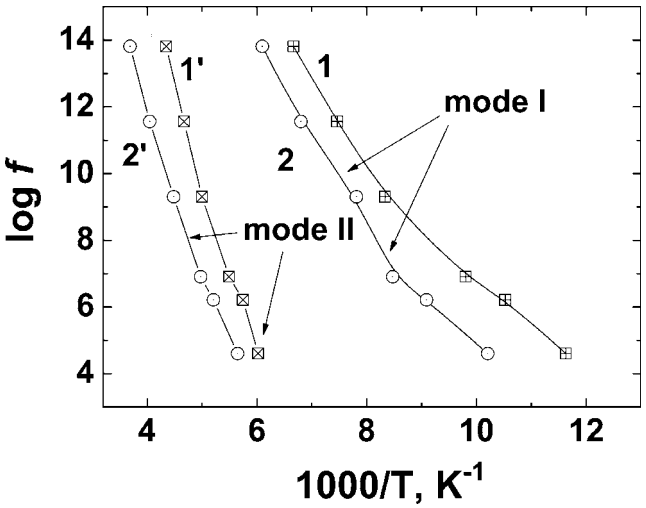

Fig. 7. Arrhenius plots for the $Ba_9CoNb_{14}O_{45}$ (1, 1′) and $Ba_9ZnNb_{14}O_{45}$ (2, 2′) relaxation modes I and II.

Table II. Fitted Relaxation Parameters (Activation Energy E_a and Preexponential Coefficient f_∞) of $Ba_9CoNb_{14}O_{45}$ and $Ba_9ZnNb_{14}O_{45}$ Ceramics

	Mode I		Mode II	
Composition	E_a (eV)	$f_\infty 0$ (Hz)	E_a (eV)	f_∞ (Hz)
$Ba_9CoNb_{14}O_{45}$	0.16	7.9×10^{10}	0.47	1.05×10^{16}
$Ba_9ZnNb_{14}O_{45}$	0.19	1.3×10^{11}	0.40	1.03×10^{13}

denote the presence of two different mechanisms responsible for the dielectric relaxation in the $Ba_9M^{2+}Nb_{14}O_{45}$ ceramics. Previously, the presence of several different relaxation modes have been reported for the $Cd_2Nb_2O_7$ ceramics,[18] although the authors did not present any clear explanation of this phenomenon.

It is interesting to note that the parameters presented in Table II are close enough to those calculated for different relaxation modes in $Cd_2Nb_2O_7$.[18] Nevertheless, we can only assume that the origin of both mechanisms found in $Ba_9M^{2+}Nb_{14}O_{45}$ derives probably from the structural disorder in the TTB crystal lattices. This disorder is associated with the different size of the cations residing in the equivalent crystallographic sites. Obviously, structural disorder is the main contribution to the relaxation found in $Ba_9M^{2+}Nb_{14}O_{45}$, and hence to the associated high dielectric loss. However, the understanding of these processes requires the further study of the dielectric parameters at higher frequencies up to microwave and optical ranges. Moreover, taking into account the fact that the $Ba_9M^{2+}Nb_{14}O_{45}$ are the main secondary phases contributing to the microwave losses of the ordered perovskites $Ba(M^{2+}{}_{1/3}Nb_{2/3})O_3$ (M^{2+} = Mg, Co, Zn), any further evaluation of the microwave characteristics of studied TTB phases seems to be of a high relevance.

IV. Conclusions

Crystal phases with the tetragonal tungsten bronze (TTB) structure are often present in the microwave dielectric ceramics based on Ba-deficient perovskites $Ba(M^{2+}{}_{1/3}Nb_{2/3})O_3$ (M^{2+} = Mg, Co, Zn). However, the effect of these TTB phases on the properties of a ceramic material was not yet clearly understood. In our study, we confirmed the sole formation of the 9:1:7 TTB compounds $Ba_9MNb_{14}O_{45}$ in the vicinity of 3:1:1 perovskite $Ba(M^{2+}{}_{1/3}Nb_{2/3})O_3$ (M^{2+} = Mg, Co, Zn) and for the first time, reported on the dielectric properties of near single-phase 9:1:7 TTB ceramics. All of the studied materials exhibit high values of dielectric permittivity (ε = 800–1100) together with its strong frequency dispersion accompanied by the monotonic rise of dielectric loss. The dielectric spectra of $Ba_9M^{2+}Nb_{14}O_{45}$ demonstrate a typical relaxor behavior. At low temperatures (100–300 K), two relaxation modes have been found in the tan δ (T) dependence of $Ba_9M^{2+}Nb_{14}O_{45}$, which can be associated with two different mechanisms of structural disorder in the TTB crystal lattice. Dielectric relaxation found in $Ba_9MNb_{14}O_{45}$ materials can be the main factor responsible for the increasing dielectric loss in Ba-deficient perovskites $Ba(M^{2+}{}_{1/3}Nb_{2/3})O_3$.

References

[1]M. T. Sebastian, *Dielectric Materials for Wireless Communication*. Elsevier Science, Oxford, U.K., 2008.

[2]H. Hughes, D. M. Iddles, and I. M. Reaney, "Niobate-Based Microwave Dielectrics Suitable for Third Generation Mobile Phone Base Stations," *Appl. Phys. Lett.*, **79** [18] 2952–4 (2001).

[3]T. Kolodiazhnyi, A. Petric, A. Belous, O. V'yunov, and O. Yanchevsky, "Synthesis and Dielectric Properties of Barium Tantalates and Niobates with Complex Perovskite Structure," *J. Mater. Res.*, **17** [12] 3182–9 (2002).

[4]A. Belous, O. Ovchar, O. Kramarenko, D. Mischuk, B. Jancar, M. Spreitzer, G. Annino, D. Grebennikov, and P. Mascher, "Low-Loss Perovskite Niobates $Ba(M^{2+}{}_{1/3}Nb_{2/3})O_3$: Composition, Structure, and Microwave Dielectric Properties," *Ferroelectrics*, **387**, 36–45 (2009).

[5]T. Kolodiazhnyi, G. Annino, and T. Shimada, "Intrinsic Limit of Dielectric Loss in Several $Ba(B_{1/3}B_{2/3})O_3$ Ceramics Revealed by the Whispering-Gallery Mode Technique," *Appl. Phys. Lett.*, **87**, 212908 (1–3) (2005).

[6]S. Desu and H. M. O'Bryan, "Microwave Loss Quality of $Ba(Zn_{1/3}Nb_{2/3})O_3$," *J. Am. Ceram. Soc.*, **68** [10] 546–51 (1985).

[7]M. A. Akbas and P. K. Davies, "Ordering-Induced Microstructures and Microwave Dielectric Properties of the $Ba(Mg_{1/3}Nb_{2/3})O_3$–$BaZrO_3$ System," *J. Am. Ceram. Soc.*, **81** [3] 670–6 (1998).

[8]H. Wu and P. K. Davies, "Influence of Non-Stoichiometry on the Structure and Properties of $Ba(Zn_{1/3}Nb_{2/3})O_3$ Microwave Dielectrics: II. Compositional Variations in Pure BZN," *J. Am. Ceram. Soc.*, **89** [7] 2250–63 (2006).

[9]O. Ovchar, A. Belous, O. Kramarenko, D. Mischuk, B. Jancar, M. Spreitzer, G. Annino, D. Grebennikov, and P. Mascher, "The Effect of Impurity Phases on the Structure and Properties of Microwave Dielectrics Based on Complex Perovskites $Ba(M_{1/3}{}^{2+}Nb_{2/3})O_3$," *Ferroelectrics*, **387**, 189–96 (2009).

[10]H. Zhang, L. Fang, and B. Wu, *PDF 50-1884*. State Key Lab. for Adv. Tech. for Mater. Synthesis And Processing. Wuhan University of Technology, China, *ICDD Grant-in Aid*, Newtown Square, PA 1999.

[11]H. Zhang, L. Fang, and L. Qin, *PDF 51-1869*. State Key Lab. for Adv. Tech. for Mater. Synthesis And Processing, Wuhan University of Technology, China, *ICDD Grant-in Aid*, Newtown Square, PA 2000.

[12]M. C. Foster, G. R. Brown, R. M. Nielson, and S. C. Abrahams, "$Ba_6CoNb_9O_{30}$ and $Ba_6FeNb_9O_{30}$: Two New Tungsten-Bronze-Type-Like Ferroelectrics," *J. Appl. Cryst.*, **30**, 495–501 (1997).

[13]P. P. Liu, X. L. Zhu, and X. M. Chen, "Relaxor Ferroelectric and Magnetic Properties of $Ba_6CoNb_9O_{30}$ Ceramics with Tungsten Bronze Structure," *J. Appl. Phys.*, **106**, 074111, 4pp (2009).

[14]T. Kolodiazhnyi, A. Belik, T. Ozawa, and E. Takayama-Muromach, "Phase Equilibria in the BaO–MgO–Ta_2O_5 System," *J. Mater. Chem.*, **19**, 8212–5 (2009).

[15]S. M. Gupta, E. Furman, E. Colla, Z. Xu, and D. Viehland, "Relaxational Polarization in Polar Dielectric Barium Magnesium Niobate," *J. Appl. Phys.*, **88** [5] 2836–42 (2000).

[16]T. Kolodiazhnyi, K. Fujita, L. Wang, Y. Zong, K. Tanaka, Y. Sakka, and E. Takayama-Muromachi, "Magnetodielectric Effect in $EuZrO_3$," *Appl. Phys. Lett.*, **96**, 252901 (1–3) (2010).

[17]S. Kamba, V. Porokhonskyy, A. Pashkin, V. Bovtun, J. Petzelt, J. C. Nino, S. Trolier-McKinstry, M. T. Lanagan, and C. A. Randall, "Anomalous Broad Dielectric Relaxation in $Bi_{1.5}Zn_{1.0}Nb_{1.5}O_7$ Pyrochlore," *Phys. Rev. B*, **66** [5] 054106, 8pp (2002).

[18]C. Ang, R. Guo, A. S. Bhalla, and L. E. Cross, "Dielectric Relaxation Processes in $Cd_2Nb_2O_7$ Compound," *J. Appl. Phys.*, **87** [10] 7452–6 (2000).